Structural Investigations on Hybrid Polymers Suitable as a Nanoparticle Precipitation Environment

Claudia Feldgitscher,[†] Herwig Peterlik,[‡] Michael Puchberger,[†] and Guido Kickelbick*,[†]

Institute of Materials Chemistry, Vienna University of Technology, Getreidemarkt 9, 1060 Vienna, Austria, and Faculty of Physics, University of Vienna, Strudlhofgasse 4, 1090 Vienna, Austria

Received August 8, 2008. Revised Manuscript Received November 21, 2008

Cross-linked hybrid polymer matrices with tunable hydrophilic/hydrophobic areas were prepared from end-group functionalized poly(ethylene oxides) (PEO) and poly(methylhydrido siloxanes) (PMHS) or trimethylsilyl terminated polydimethyl-co-polymethylhydrido siloxanes (PDMS-PMHS). The combination of the different polymer segments resulted in materials with hydrophilic and metal coordinating sections in a hydrophobic matrix. The polymer morphology was investigated with regard to its chemical composition and structural configuration. Besides spectroscopic methods, DSC and swelling tests were performed to study the chain mobility in the polymer matrix. The cross-linked polymers were swellable in methanol, reaching swelling degrees of up to 550%. On the basis of the excellent swelling behavior and the unique metal ion binding ability of the PEO segments, hybrid nanocomposites were prepared infiltrating the matrix with iron ions and forming nanocrystalline oxide particles in the cross-linked network. The resulting materials were analyzed by electron microscopy techniques, XRD, and small-angle X-ray scattering.

Introduction

Controlled embedment of nanoparticles in designed and tunable polymer matrices are the basis for a wide range of applications in bio- and nanochemistry.[1] In recent years, research in this field focused particularly on magnetic nanoparticles created inside of preformed cavities, biological templates, or matrix-assisted assemblies. Examples of the former include ferritin protein coat and viral protein cages,[2] whereas examples of the latter comprise zeolites,[3] polyimine, and organosilicas.[4] The understanding of the polymer structure is crucial for the matrix-assisted formation of nanoparticles in polymer networks. A prominent polymeric material used in the preparation of inorganic−organic nanocomposites is formed by the combination of poly(ethylene oxide) (PEO) with polysiloxanes. The most striking properties of these hybrid polymers are ion binding and ion conducting ability, chemical stability, and amphiphilic character.[5−9] The synthetic strategy often applied in the formation of PEO-polysiloxane materials is the grafting of end-group-functionalized PEOs to polysiloxane backbones via hydrosilation.[7] This method is, for example, used in the preparation of solid polymer electrolytes (SPE). Although the thus formed polymers consist of PEO chains pending from a polysiloxane backbone, novel cross-linked systems show a unique ion conducting character.[8−11] In the reported literature, almost no attention was given to the ion binding ability of these polymers and the use of such matrices for the in situ formation of nanoparticles. Furthermore, in the reported studies, the two usually immiscible components are linked by either a third moiety acting as a cross-linker or by the preparation of a linear precursor and the subsequent formation of the cross-links via sol−gel reactions.[12,13] Earlier works described, for example, the preparation of PEO/polysiloxane networks via zinc octoate catalyzed reactions. However, in these studies, hydrolytic sensitive Si−O−C bonds were formed which make these polymers sensitive to a water-based precipitation chemistry inside of the cross-linked matrices. Such an unstable linkage between the two components is also built by self-condensation or alkoxy exchange.[14] The Pt-catalyzed hydrosilation reaction creates an alternative pathway towards the formation of ion conducting cross-linked PEO/polysiloxane systems[15] leading to the synthesis of chemically and thermally stable cross-linked polymers.

* Corresponding author. E-mail: guido.kickelbick@tuwien.ac.at.
[†] Vienna University of Technology.
[‡] University of Vienna.

(1) Vaia, R. A.; Maguire, J. F. *Chem. Mater.* **2007**, *19*, 2736–2751.
(2) Douglas, T.; Dickson, D. P. E.; Betteridge, S.; Charnock, J.; Garner, C. D.; Mann, S. *Science* **1995**, *269*, 54–7.
(3) Cowen, J. A.; Tsai, K. L.; Dye, J. L. *J. Appl. Phys.* **1994**, *76*, 6567–9.
(4) Rao, M. S.; Dubenko, I. S.; Roy, S.; Ali, N.; Dave, B. C. *J. Am. Chem. Soc.* **2001**, *123*, 1511–1512.
(5) Hooper, R.; Lyons, L. J.; Moline, D. A.; West, R. *Organometallics* **1999**, *18*, 3249–3251.
(6) Zhou, G. B.; Khan, I. M.; Smid, J. *Macromolecules* **1993**, *26*, 2202–8.
(7) Zhang, R.; Zhang, Z.; Amine, K.; West, R. *Silicon Chem.* **2005**, *2*, 271–277.
(8) Kang, Y.; Lee, J.; Suh, D. H.; Lee, C. *J. Power Sources* **2005**, *146*, 391–396.
(9) Sanchez, C.; Julian, B.; Belleville, P.; Popall, M. *J. Mater. Chem.* **2005**, *15*, 3559–3592.
(10) Chaker, J. A.; Santilli, C. V.; Pulcinelli, S. H.; Dahmouche, K.; Briois, V.; Judeinstein, P. *J. Mater. Chem.* **2007**, *17*, 744–757.
(11) Walcarius, A.; Mandler, D.; Cox, J. A.; Collinson, M.; Lev, O. *J. Mater. Chem.* **2005**, *15*, 3663–3689.
(12) Dahmouche, K.; Santilli, C. V.; Da Silva, M.; Ribeiro, C. A.; Pulcinelli, S. H.; Craievich, A. F. *J. Non-Cryst. Solids* **1999**, *247*, 108–113.
(13) Gomes Correia, S. M.; de Zea Bermudez, V.; Silva, M. M.; Barros, S.; Sa Ferreira, R. A.; Carlos, L. D.; Smith, M. J. *Electrochim. Acta* **2002**, *47*, 2551–2555.
(14) Kuo, P.-L.; Hou, S.-S.; Lin, C.-Y.; Chen, C.-C.; Wen, T.-C. *J. Polym. Sci., Part A: Polym. Chem.* **2004**, *42*, 2051–2059.

10.1021/cm802171s CCC: $40.75
Published on Web 01/22/2009

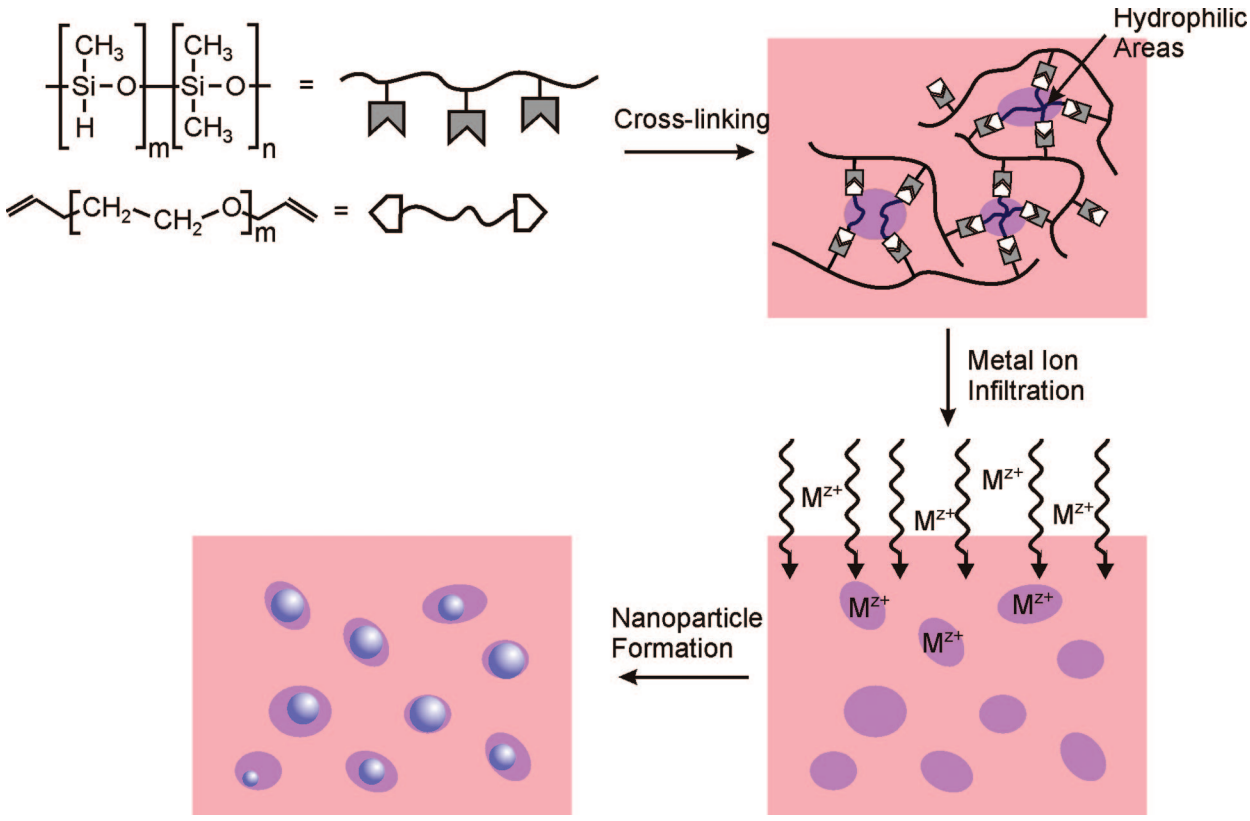

Figure 1. Formation of the hybrid PEO-polysiloxane matrix and use of this cross-linked polymer for the in situ preparation of nanoparticles.

The preparation of nanoparticle containing hybrid polymers is usually performed via two different pathways, either the mixing of the nanoparticles with the monomers followed by polymerization[16,17] or the formation of the nanoparticles during polymerization.[18] In this work, we present a novel route in the preparation of nanocomposites applying a swollen cross-linked polymer matrix as the precipitation environment of nanoparticles. Three different types of hybrid polymer matrices were structurally investigated: (i) a PMHS backbone or (ii) a PDMS-PMHS block copolymer backbone cross-linked by diallyl-terminated PEO and (iii) additionally modified systems with end-group functionalized oligo ethylene glycol methyl ethers. The resulting materials were used as matrices for the formation of iron oxide nanoparticles (Figure 1).

Experimental Section

Measurements. Relative size exclusion chromatography (SEC) measurements in tetrahydrofuran were performed using a Waters system including a 515 HPLC pump, a 717 autosampler, a 2410 differential refractive index detector, and Styragel columns (HR 0.5, 3, and 4, linear and GPC PHASE SDV 50/100/10E5A) at 40 °C and a rate of 1 mL/min, applying linear polystyrene standards. Molecular weight analyses were carried out using Waters Millennium software including the GPC/V option and were related to an internal standard (biphenyl ether). Solution NMR spectra were recorded on a Bruker Avance 250 instrument (^{1}H at 250 MHz, ^{13}C at 75 MHz). Solid state NMR spectra were recorded on a Bruker Avance 300 instrument equipped with a 4 mm broadband MAS probe head operating at 75.43 and 59.6 MHz for ^{13}C and ^{29}Si, respectively. ^{13}C spectra were recorded with ramped CP/MAS spectra (cross polarization and magic angle spinning), whereas ^{29}Si spectra were recorded with HPDEC (high power decoupling). The rotor spinning speed was usually 6−8 kHz.

TGA was carried out applying a Netzsch TG 209c in synthetic air and the data were processed using Netzsch Proteus Analysis Software. DSC measurements were performed on a DSC823^e with liquid nitrogen cooling from Mettler Toledo. The polymer samples were powdered and filled into 40 μL aluminum crucibles. Measurements were carried out under N_2 atmosphere and a typical temperature program consisted of cooling with 10 °C/min to −150 °C a holding time of 5 min and a subsequent heating with 10 °C/min to 180 °C.

IR spectra were recorded with a Bruker Tensor 27 with an ATR micro focusing MVP-QL.

Small-angle X-ray measurements were performed with a rotating anode generator (Nanostar, Bruker-AXS), equipped with a pinhole camera, and Cu Kα radiation collimated and monochromatized from crossed Göbel mirrors. All X-ray patterns were radially averaged and corrected for background scattering to obtain the scattering intensity in dependence on the scattering vector q, where $q = 4\pi\sin\theta/\lambda$ with 2θ being the scattering angle and $\lambda = 0.1542$ nm the X-ray wavelength. The measurements were performed at two different specimen-to-detector distances (1.05 and 0.13 m) to cover a wide range of the scattering vector. In the diagrams, only the data in the range between $q = 2$ and 18 nm^{-1} are shown, where the main structural features are visible.

(15) Zhang, Z.; Sherlock, D.; West, R.; West, R.; Amine, K.; Lyons, L. J. *Macromolecules* **2003**, *36*, 9176–9180.
(16) Balazs, A. C.; Emrick, T.; Russell, T. P. *Science* **2006**, *314*, 1107–1110.
(17) Baker, C.; Ismat Shah, S.; Hasanain, S. K. *J. Magn. Magn. Mater.* **2004**, *280*, 412–418.
(18) Guermeur, C.; Lambard, J.; Gerard, J.-F.; Sanchez, C. *J. Mater. Chem.* **1999**, *9*, 769–778.

The crystallinity and the phase composition of the samples were examined by powder diffractometry (XRD) on a Philips X'Pert diffractometer using the Cu Kα line as X-ray source.

TEM measurements were performed on a JEOL JEM-100CX at the University Service Centre for Transmission Electron Microscopy, Vienna University of Technology, Austria.

Scanning electron microscopy (SEM) images were recorded on a Philips XL-30. The samples were sputtered on the surface with a thin gold layer prior to SEM imaging. The typical measurement conditions (accelerating voltage, magnification, etc.) are mentioned on the images.

For swelling degree determination, the weighted samples were transferred in a desiccator containing an open vessel with the swelling agent to guarantee an equilibrium atmosphere. Solvents studied were water, toluene, acetonitrile, and methanol. The polymers were weighted after appropriate periods of time. Empty vials were also placed in the desiccator and weighted as well to minimize the systematic error. The desiccator was transferred into a furnace that was set to 40 °C for analysis of the swelling degree. The sample weight was measured by either balance weighting, the determination of the mass loss at 35 °C, or during heating via TGA. The sample mass was determined gravimetrically and calculated according to the following equation

$$\text{Swelling degree} = \frac{m_s - m_d}{m_d} 100$$

where m_s = mass of the swollen sample and m_d = mass of the dried sample.

Chemicals. THF and toluene were distilled over sodium and stored under an argon atmosphere. Allyl bromide (Aldrich) was distilled under vacuum before use. Solutions of bis(1,3-divinyl,1,1,3,3-tetramethyldisiloxane) Pt(0) (Karstedt catalyst) (Aldrich) were prepared in absolute toluene or THF (2 mM). Trimethylsilyl-terminated poly(dimethyl-co-polymethylhydrido siloxane) (PDMS-PMHS), poly(methylhydrido siloxane) (PMHS), diethyleneglycol mono methyl ether, triethylene glycole mono methyl ether and poly(ethylene oxide) (PEO) of different chain lengths (M_w = 300, 400, 500, 600 g/mol) were received from Aldrich and used without further purification.

Sample Preparation. *Preparation of α,ω-Diallyl Poly(ethylene oxides) (aPEO).* α,ω-Diallyl poly(ethylene oxides) of different chain lengths were prepared using hydroxy terminated poly(ethylene oxides) (M_w = 200, 300, 400, 600, 1000 g/mol) as precursors. The preparation procedure was adopted from the literature:[19] 30.0 g (50 mmol) of poly(ethylene oxide) (M_w = 600 g/mol) was dissolved in 50 mL of abs. THF; 11.2 g of fine crunched KOH (4 equiv., 200 mmol) was added and stirred with a magnetic stirrer at room temperature in a 250 mL three-neck round-bottom flask equipped with a condenser and a dropping funnel for 30 min. The distilled allyl bromide (19.4 g, 3.2 equiv., 160 mmol) was dissolved in 15 mL of abs. THF and added dropwise via a dropping funnel. After addition of the allyl bromide, the reaction mixture was heated to reflux for 12 h. The thus obtained yellow oil was filtrated, washed three times with 2N NaOH, and dried over Na_2SO_4. Characterization based on α,ω-diallyl poly(ethylene oxides) (aPEO, starting from M_w = 600 g/mol): yield, 25.7 g (76%); GPC-result, M_w = 660, M_w/M_n = 1.11.

ATR-FTIR ν (cm^{-1}): 847 (νCO, rCH_2), 928 (νCO, rCH_2), 1039 (νCO, νCC, rCH_2), 1097 (νCO), 1250 (CH_2 twisting), 1295 (CH_2 twisting), 1349 (CH_2 wagging), 1458 (CH_2 scissoring), 1646 (CH_2=CH), and 2865 (νsCH_2).

^{1}H NMR δ ($CDCl_3$, ppm): 5.88 (m, 1H, CH_2CH CH_2), 5.22 (dd, 2H, J = 13.5 Hz, J = 10 Hz CH_2CHCH_2), 4.00 (d, 2H, J = 2.8 Hz, CH_2CH CH_2), 3.65 (s, 25H, CH_2CH_2O−).

^{13}C NMR δ ($CDCl_3$, ppm): 134.6 (CH_2=CH), 116.4 (CH_2=CH), 71.6 (CH_2=CH−CH_2), 70.3 (O−CH_2−CH_2−O), 69.1 (CH_2−OH), 58.5 (OCH_3).

Preparation of the Monofunctionalized PEO. The preparation of the monofunctionalized PEO (starting from diethylene glycol mono methyl ether, triethylene glycol mono methyl ether) follows a procedure similar to that for the α,ω-diallyl poly(ethylene oxides).

A total of 9.7 g (50 mmol) of triethylene glycole mono methyl ether was dissolved in 30 mL of absolute THF; 5.6 g of fine crunched KOH (4 equiv., 100 mmol) was added and stirred with a magnetic stirrer at room temperature in a 250 mL three neck round-bottom flask equipped with a condenser and a dropping funnel for half an hour. The distilled allyl bromide (7.87 g, 1.3 equiv., 65 mmol) was dissolved in 10 mL of abs. THF and added dropwise via a dropping funnel. After addition of the allyl bromide the reaction mixture was heated to reflux for 12 h. The thus obtained yellow oil was filtrated, washed three times with 2N NaOH, and dried over Na_2SO_4. Characterization based of the modified triethylene glycole mono methyl ether: yield, 8.4 g (72%); GPC-result, M_w = 240, M_w/M_n = 1.02.

ATR-FTIR ν (cm^{-1}): 851 (νCO, rCH_2), 924 (νCO, rCH_2), 995 (νCO, rCH_2), 1027 (νCO, νCC, rCH_2), 1104 (νCO), 1199 (CH_2 twisting), 1248 (CH_2 twisting), 1294 (CH_2 twisting), 1350 (CH_2 wagging), 1454 (CH_2 scissoring), 1645 (CH_2=CH), 2870 (νsCH_2), 2970 (νaCH_3).

^{1}H NMR δ (ppm, $CDCl_3$): 5.79 (*m*, 1.0*H*, CH_2=C*H*−), 5.13 (*dd*, 2.0*H*, J = 21.3, J = 28.2, CH_2=CH−), 3.91 (*d*, 2.0*H*, J = 5.6 Hz, CH_2=CH−CH_2−), 3.56 (*m*, 14*H*, −O−CH_2CH_2−O−), 3.27 (*s*, 3.0*H*, −O−CH_3).

^{13}C NMR δ (CDCl3, ppm): 134.6 (CH_2=*C*H), 116.8 (*C*H_2=CH), 71.9 (*C*H_2=CH−*C*), 70.3 (O−*C*H_2−CH_2−O), 69.2 (CH_2−OH).

Preparation of the Cross-Linked Hybrid Polymers. All hydrosilation reactions were carried out in flame-dried Schlenk tubes under Ar atmosphere and were handled under Ar. The ratios between α,ω-diallyl poly(ethylene oxides) (aPEO) and PDMS-PMHS (polydimethyl-co-polymethylhydrido siloxane trimethylsilyl terminated (M_w = 950 g/mol)) or PMHS (polymethylhydridosiloxane (M_w = 1700−3200 g/mol)) were varied, resulting in polymers showing EO:Si ratios starting from 0.06 up to 5.68. Si−H to doublebond ratios were varied from 35:1 to 1:1. aPEO of different molecular masses were applied (M_w= 284, 384, 484, 684, 1084 g/mol). Either abs. toluene or abs. THF was used as solvent.

A typical preparation procedure was as follows: 0.48 g of PDMS-PMHS (0.5 mmol, 1 equiv.) and 0.77 g aPEO (1.13 mmol, 2.26 equiv.) were dissolved in 15 mL of THF in a Schlenk flask. A solution of Karstedt catalyst in THF (2 mM) was prepared and 1 mL of this catalyst solution was added to the mixture. Gelation times were determined optically and recorded. The solvent was evaporated and the cross-linked polymer dried in a vacuum. Yield: 0.9 g (72%).

Characterization based on the cross-linked polymer sample starting from PDMS-PMHS:PMHS2-PEO6 2.21 (EO:Si).

ATR-FTIR ν (cm^{-1}): 694 (C−Si−C), 797 (C−Si−C), 847 (νCO, rCH_2), 908 (Si−H), 1025 (νCO, νCC, rCH_2, Si−O−Si), 1084 (νCO), 1258 (νSi-CH_3, CH_2 twisting), 1295 (CH_2 twisting), 1351 (CH_2 wagging), 1456 (CH_2 scissoring) 2165 (Si−H) 2869 (νsCH_2) and 2952 (νaCH_3).

^{13}C CP/MAS δ (25 °C, ppm): 66.4 (OCH_2CH_2O), 63.7 (OCH_2CH_2O), 16.4 ($CH_2CH_2CH_2$O), 6.5 (Si−CH_2−CH_2), −5.9 (Si−CH_3), −7.3 (Si−CH_3), −9.5 (H−Si−CH_3).

(19) Mitchell, T. N.; Heesche-Wagner, K. *J. Organomet. Chem.* **1992**, *436*, 43–53.

^{29}Si HPDEC/MAS δ (25 °C, ppm): 7.9 ($(CH_3)SiO$, M^1), −21.5 ($OSi(CH_3)_2$, D^1), −37.1 ($OSi(CH_3)H$, D^H), −57.7 (SiO_3CH_3, T^2), −67.1 (SiO_3CH_3, T^3).

Characterization based on the cross-linked polymer sample starting from PMHS:

PMHS1-PEO6 0.19 (EO:Si).

ATR-FTIR ν (cm^{-1}): 759 (C−Si−C), 796 (C−Si−C), 851 (νCO, rCH_2), 896 (Si−H), 1027 (νCO, νCC, rCH_2, Si−O−Si), 1090 (shoulder, νCO), 1262 (νSi-CH_3, CH_2 twisting), 1303 (CH_2 twisting), 1354 (CH_2 wagging), 1454 (CH_2 scissoring) 2164 (Si−H) 2871 (νsCH_2) and 2964 (νaCH_3).

^{13}C CP/MAS δ (25 °C, ppm): 66.3 (OCH_2CH_2O), 63.8 (OCH_2CH_2O), 16.25 ($CH_2CH_2CH_2O$), 6.4 ($Si-CH_2-CH_2$), 0.03 ($(Si-CH_3)_3$), −9.5 ($H-Si-CH_3$).

^{29}Si HPDEC/MAS δ (ppm): 7.6 ($(CH_3)SiO$, M^1), −22.0 ($OSi(CH_3)_2$,D^1), −38.1 ($OSi(CH_3)H$, D^H), −59.9 (SiO_3CH_3, T^2), −67.9 (SiO_3CH_3, T^3).

Functionalization of the Cross-Linked Polymer with Mono-Allyl-Functionalized Triethylene Glycol Mono Methyl Ether or Diethylene Glycol Mono Methyl Ether. Usually the pre-cross-linked polymer was used as a dried sample, but in some reactions the polymer was not removed from the reaction solution and was used for the functionalization without further drying. A typical procedure was as follows: 0.15 g of the cross-linked polymer was swollen in 10 mL of toluene for 2 h under stirring. Then, 0.095 g of diethylene glycol methyl ether (0.6 mmol) was added and left to stir for another 2 h; 0.1 mL of the catalyst solution (2 mM) was added and stirred overnight.

Characterization based on PMHS2-PEO6 1.7 (EO:Si).

ATR-FTIR ν (cm^{-1}): 688 (C−Si−C), 797 (C−Si−C), 843 (νCO, rCH_2), 1013 (νCO, νCC, rCH_2, Si−O−Si), 1088 (νCO), 1259 (νSi-CH_3, CH_2 twisting), 1295 (CH_2 twisting), 1351 (CH_2 wagging), 1454 (CH_2 scissoring), 2868 (νsCH_2) and 2959 (νaCH_3).

^{13}C CP/MAS δ (25 °C, ppm): 66.6 (OCH_2CH_2O), 63.7 (OCH_2CH_2O), 51.5 (OCH_3), 16.5 ($CH_2CH_2CH_2O$), 6.7 ($Si-CH_2-CH_2$), −5.9 ($Si-CH_3$), −7.4 ($Si-CH_3$), −9.4 ($Si-CH_3$).

^{29}Si HPDEC/MAS δ (25 °C, ppm): 8.4 ($(CH_3)SiO$, M^1), −18.3 ($OSi(CH_3)_2$, D^1), −20.9 ($OSi(CH_3)_2$, D^1), −56.7 (SiO_3CH_3, T^2).

Infiltration with $FeCl_3$ and $FeCl_2$ Solutions. Polymers were infiltrated with $FeCl_3$ and $FeCl_2$ solutions. A typical procedure was as follows: Dried polymers were placed for 16 h in a $FeCl_3$ solution (0.25 M/H_2O), and the supernatant solution was then decanted and the polymer washed three times with water. Afterwards, an aqueous ammonia solution (0.5 M/H_2O) was added. After 12 h the supernatant solution was decanted and the polymer was washed three times with water. The polymers were dried in a vacuum.

ATR-FTIR ν (cm^{-1}): 700 (C−Si−C), 800 (C−Si−C), 849 (νCO, rCH_2), 1021 (νCO, νCC, rCH_2, Si−O−Si), 1085 (νCO), 1259 (νSi-CH_3, CH_2 twisting), 1350 (CH_2 wagging), 1412, 1454 (CH_2 scissoring), 1643, 2867 (νsCH_2), 2958 (νaCH_3), and 3360 (OH).

Results and Discussion

Preparation of Cross-Linked Polymers. Inorganic−organic hybrid polymers were prepared by the hydrosilation reaction of aPEO with linear polysiloxanes in a specific EO:Si ratio. Various polymer morphologies were achieved using two different types of polysiloxanes, namely PMHS and PDMS-PMHS (see Figure 1). The homopolymer PMHS offers approximately 35 Si−H units per macromolecule whereas the PDMS-PMHS contains only 5 Si−H units, located in one segment of the block copolymer. The Si−H groups of both polymer types were used for the Pt-catalyzed hydrosilation reactions with allyl-modified PEOs. The resulting cross-linked polymers are distinguished by their structural ordering and morphology.

PMHS acts as a polymer backbone that provides many functional groups for cross-linking the single chains with PEO molecules (Figure 2a) resulting in a brittle material. Contrary, the block copolymer PDMS-PMHS is able to form cross-links with only one segment of the polysiloxane chain. Cross-linking PEO chains are located in close vicinity to one another and only weak interactions of the dangling PDMS parts are expected, leading to a soft and rubbery polymer material (Figure 2b). Thus different cross-linking densities were obtained applying the different polymers. In previous studies, we could show that the morphology of PDMS-PMHS chains in solution depends on the interaction of the polymer with the solvent.[20] The macromolecules tend to form coil-like structures and bundles if a nonsolvent, such as ethanol, is used or spread to their linear form if a good solvent, like toluene, is applied.

The cross-linking density has two consequences for the properties of the final materials: (i) a different swelling behavior, and (ii) the PEO to polysiloxane ratio induces changing hydrophobic/hydrophilic properties in the polymers.

The hydrosilation reaction was carried out in absolute toluene or THF using Schlenk technique applying the Karstedt catalyst.[21] The amount of catalyst per Si−H was kept at 0.02 mol/mol Si−H, hence the catalyst concentrations was in the range of 0.33−3.3 mmol/L. Telechelic allyl PEO with 5, 13, and 25 EO units per chain were prepared via a coupling reaction of allyl bromide with the OH-terminated PEO in high yields[19] and used in the cross-linking reactions. When this procedure was applied, materials with varying EO:Si ratios were obtained (0.06−5.68). In the following descriptions, polymers resulting from PMHS are assigned with PMHS1 and polymers bearing a PDMS-PMHS backbone are assigned with PMHS2. The use of a PEO with, for example, 200 g/mol is indicated in the resulting polymer with PEO2. The EO:Si ratio is given as the number following the types of polysiloxane and PEO used (Table 1).

In terms of application of these polymer matrices as the precipitation environment of nanoparticles, the number of ion binding sites was increased by the additional introduction of allyl end-group-functionalized diethylene glycole monomethylether or triethylene glycole monomethylether that were not able to induce further cross-linking (Figure 2c). These functionalities were reacted with residual Si−H groups in already cross-linked polymer matrices prepared from PMHS2 by hydrosilation leading to an increase of hydrophilicity. The post functionalization of the predesigned polymer was only possible in the case of the PMHS2 systems, most likely because of the enhanced swelling properties of the PDMS-PMHS polymers in toluene.

IR-spectra (see the Supporting Information) of PMHS1-PEO6 0.19 and PMHS2-PEO6 4.42 reveal the success of the cross-linking reactions by a decrease of the Si−H vibration at 2160 cm^{-1} of the linear polysiloxanes and the

(20) Ivanovici, S.; Rill, C.; Koch, T.; Puchberger, M.; Kickelbick, G. *New J. Chem.* **2008**, *32*, 1243–1252.
(21) Kickelbick, G.; Bauer, J.; Huesing, N.; Andersson, M.; Palmqvist, A. *Langmuir* **2003**, *19*, 3198–3201.

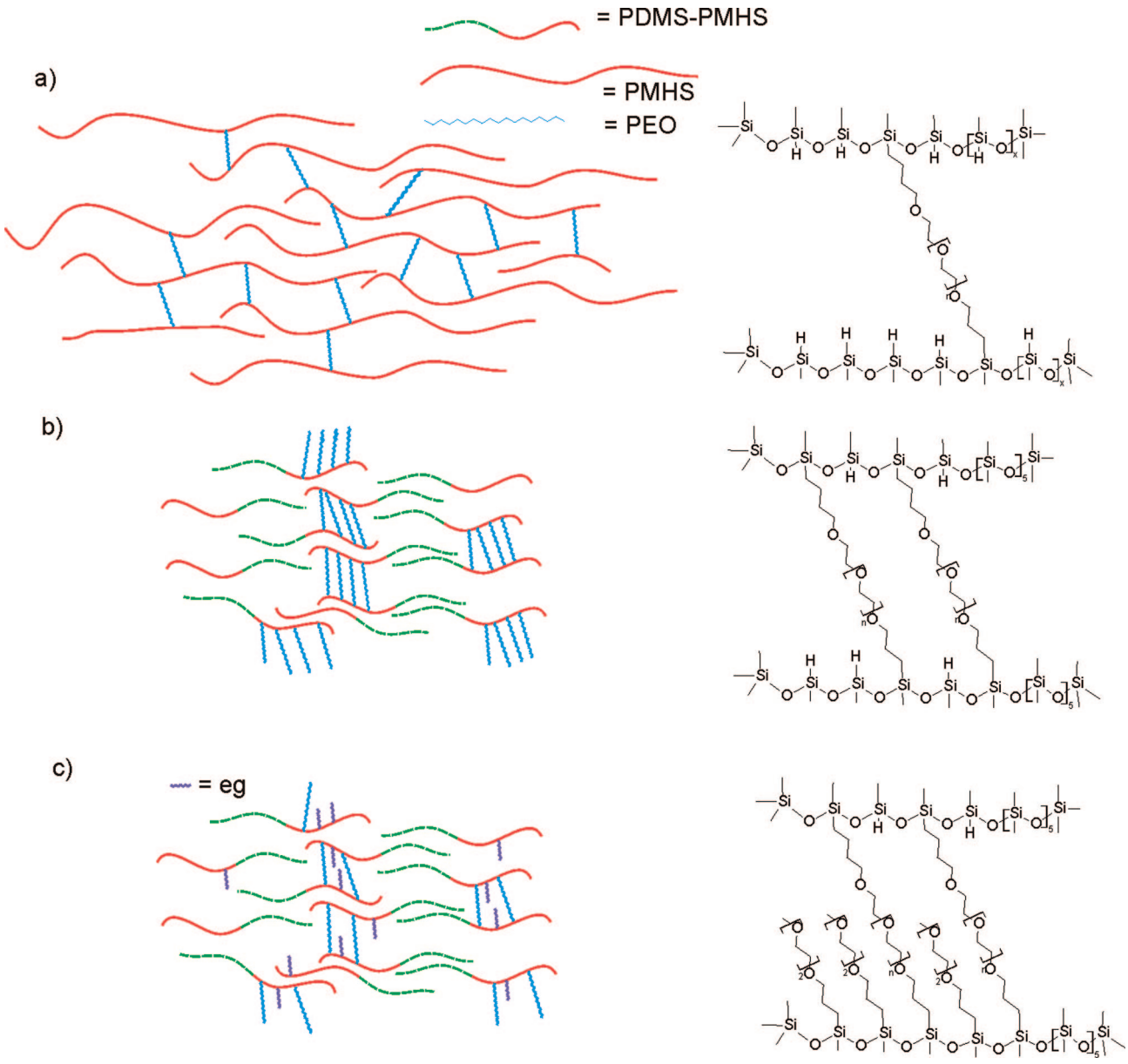

Figure 2. Schematic representation of the three types of cross-linked polymers: (a) PMHS, (b) PDMS-PMHS, (c) ethylene glycol modified cross-linked polymers.

Table 1. Selection of Polymer Samples Used in This Study

	PEO:PMHS (mol:mol)	EO:Si	wt % PEO	Additional EG (mol)
PMHS1-PEO2 0.06	1:2	0.06	5	
PMHS1-PEO6 0.19	1:2	0.19	12	
PMHS1-PEO10 1.28	2:1	1.28	47	
PMHS1-PEO6 1.51	4:1	1.51	53	
PMHS2-PEO6 2.21	2:1	2.21	59	
PMHS2-PEO6 3.31	3:1	3.3	68	
PMHS2-PEO6 4.42	4:1	4.42	74	
PMHS2-PEO6 2.71 eg	2:1	2.71	79	2
PMHS2-PEO6 3.21 eg	2:1	3.21	81	4
PMHS2-PEO6 3.71 eg	2:1	3.71	84	6

disappearance of the allyl C=C vibrations at 1646 cm^{-1} of the PEO cross-linker. The appearance of the typical double peak in the region between 1000 and 1300 cm^{-1} resulting from the C−O−C vibrations of the PEO and the Si−O vibration of the polysiloxane chain further confirms the formation of the cross-linked polymer. In the case of PMHS1-PEO6 0.19, only a peak with a shoulder is present in the same region because of the low PEO content. For samples containing oligo ethylene glycols, similar spectra were obtained. In general, no vibrations attributed to residual double bonds were found.

Further evidence for the success of the cross-linking reaction was obtained by solid-state NMR. ^{13}C CP/MAS spectra of the two different cross-linked polysiloxanes feature similar chemical shifts, therefore only the spectra of PMHS2-PEO6 2.21 are discussed in detail. The ^{13}C shifts of the cross-linking chain -OCH_2CH_2O- were found at 66.4 and 63.7 ppm. No residual allyl carbons were observed in the region between 115 and 135 ppm. The signals corresponding to the trimethyl silyl end groups were observed between −5.9 and −9.5 ppm. Samples that were additionally functionalized with ethylene glycol molecues showed the additional signal for the methoxy group at 58.5 ppm. The ^{29}Si HPDEC spectra displayed the presence of the trimethylsilyl end groups in the **M** region (7.9 ppm) and an intense signal in the **D** region

(−21.5 ppm) corresponding to the main chain Si atoms (O−Si−O). The residual Si−H functionality at −37.1 ppm had a less intense signal. In the cross-linked polymer PMHS1-PEO6 0.19 consisting of the long PMHS chain, the relative intensities of these two peaks are vice-versa, due to the higher amount of residual Si−H. Signals at −57.7 and −67.1 ppm are due to **T** type Si atoms, resulting from side products of the hydrosilation reaction (O-silylation due to moisture).[22] These side products cannot be avoided but do not interfere with the network formation.

Swelling Experiments. Chain mobilities and phase integrities were investigated using swelling experiments for a better understanding of the cross-linking degree of the hybrid polymers. Solvents were introduced into the polymers via the vapor phase to minimize surface adsorption of solvent molecules. Due to the necessity of minimization of surface effects, sample sizes were kept constant. The selection of solvents investigated in this study was based on the commonly used distinction by their polar/apolar character and with regard to further applications of the obtained materials as nanoparticle preparation matrices. On the basis of these facts, water, methanol, acetonitrile, and toluene were used as swelling agents. In addition, the development of water uptake at 40 °C was recorded. Contrary to amphiphilic conetworks,[23,24] which show hydrophilic and hydrophobic behavior simultaneously,[25] the affinity for apolar solvents does not increase with the mass percentage of polysiloxane in the cross-linked PMHS-PEO systems. Interestingly, there is an overall increase in solvent uptake when increasing the relative amount of PEO in the polymers.

In our work, polymers with low EO:Si ratios were from the type PMHS1 and polymers showing high EO:Si ratios from the block copolymer type PMHS2. In general, the different polymer systems have to be distinguished on the basis of their morphology and therefore their swelling behavior follows different mechanisms.

PMHS forms a network with randomly distributed cross-linking PEO segments throughout the whole polymer chain. Several examples of such cross-linked amphiphilic polymers or conetworks were described in the literature either by copolymerization of hydrophilic/hydrophobic polymers, e.g., starting from methacrylates going to polyisobutylene,[26] or by cross-linking of polysiloxanes with acryl amides.[27] In our case, a selection of polymer samples was investigated with EO:Si ratios ranging from 0.06 to 1.51 and cross-linked with aPEO 200, 600, and 1000. The swelling behavior for water at 40 °C and at room temperature as well as for acetonitrile showed that an increase in the siloxane content leads to a lower degree of swelling (Figure 3). This is not surprising, as water and acetonitrile are polar solvents and nonsolvents

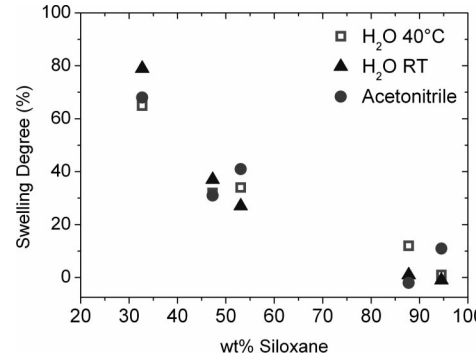

Figure 3. Swelling degree versus wt % siloxane for water at 40 °C and at room temperature and in acetonitrile.

for polysiloxanes. However, a higher uptake of toluene, which is a good solvent for polysiloxanes, was observed in dependence on time for lower siloxane contents. This leads to the conclusion that the obtained cross-linked polysiloxanes do not show typical amphiphilic behavior. The miscibility of the two components polysiloxane/PEO was investigated in the literature previously,[28] indicating structural heterogeneity. SAXS measurements, presented in the next section, indicate that the siloxane chains form entangled clusters allowing only solvent interactions with the polysiloxane aggregates located at the boundaries of the clusters. A large number of hydrophobic groups do not contribute to the polymer system, as they are effectively shielded.

Polymer networks formed with PDMS-PMHS were prepared at higher EO:Si ratios, thus more cross-links per Si−H units were obtained, resulting in a mechanically stable polymer. Here, cross-linking occurs in only one segment of the PDMS-PMHS backbone. The swelling degree of the obtained materials was higher than for the samples prepared from the PMHS homopolymer, because of the higher elasticity of the polymer system and the resulting enhanced availability of the polymer chains for interaction with solvent molecules. Hence, the polymer swelling behavior is dependent on the polymer morphology and is dominated by the PEO chain content.

With respect to further application of these cross-linked polymers as matrices for the precipitation of nanoparticles, additional functional groups with hydrophilic and coordination properties were introduced, such as allyl end-group-functionalized diethylene glycol or triethylene glycol mono methyl ethers. Thus, the hydrophilicity and metal coordination ability of the polymer was enhanced without creating further cross-links. Solvent uptake tests again showed that high EO:Si ratios led to high amounts of incorporated solvent, even for apolar molecules such as toluene (see the Supporting Information). This leads to the conclusion that contrary to the PMHS1 systems the hydrophobic moieties in the cross-linked block copolymer are still available for interactions with apolar solvents. Furthermore, the observed high swelling degree for almost all of the additionally functionalized samples indicates a polymer matrix with a high flexibility. In contrast the polymer matrices formed by

(22) Kim, B.-H.; Cho, M.-S.; Woo, H.-G. *Synlett* **2004**, 761–772.
(23) Sandro, S. L.; Ivan, B.; Scherble, J.; Mülhaupt, R.; Thomann, R. *Polym. Prepr. (Am. Chem. Soc., Div. Polym. Chem.)* **2006**, *47* (2), 1154–1155.
(24) Erdodi, G.; Kennedy, J. P. *J. Polym. Sci., Part A: Polym. Chem.* **2005**, *43*, 4953–4964.
(25) Erdodi, G.; Kennedy, J. P. *Prog. Polym. Sci.* **2006**, *31*, 1–18.
(26) Toman, L.; Janata, M.; Spevacek, J.; Brus, J.; Sikora, A.; Latalova, P.; Holler, P.; Vlcek, P.; Dvorankova, B. *J. Polym. Sci., Part A: Polym. Chem.* **2006**, *44*, 6378–6384.
(27) Erdodi, G.; Kennedy, J. P. *J. Polym. Sci., Part A: Polym. Chem.* **2006**, *45*, 295–307.
(28) Liang, W.-J.; Kao, H.-M.; Kuo, P.-L. *Macromol. Chem. Phys.* **2004**, *205*, 600–610.

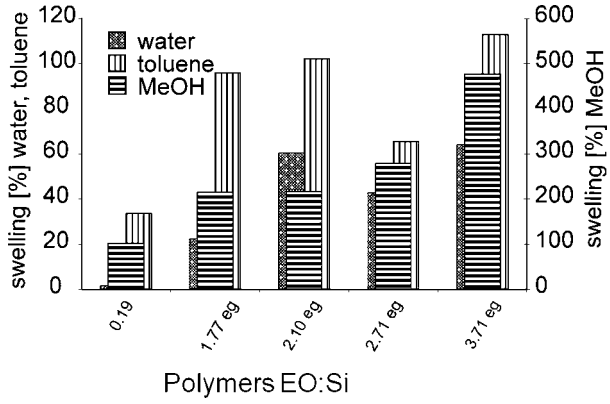

Figure 4. Solvent uptake for different types of polymers.

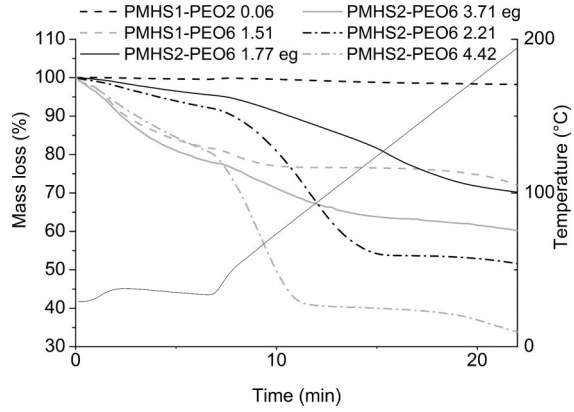

Figure 5. TGA curves of water swollen polymers: isothermal step at 35 °C.

PMHS as polysiloxane show only a very low solvent uptake even for the proper solvents for the linear PMHS chains, such as toluene (Figures 4 and 5).

The highest solvent uptake was observed for methanol, which is most likely due to the small molecular size of methanol and the possibility for the formation of hydrogen bonds which allow for excellent interactions with the PEO segments. Interestingly, PDMS-PMHS and PMHS are not soluble in methanol and thus the swelling behavior of the hybrid polymer is mainly dominated by the PEO moieties.

In addition to simple solvent uptake experiments, solvent release was measured under isothermal conditions and during heating. The time dependent water loss was determined by TG analysis in the isothermal step at 35 °C. For the samples featuring a very low EO:Si ratio (0.06), no change in the mass loss curve was observed in the isothermal step, indicating that almost no water was incorporated. As a general characteristic polymers prepared from the PMHS precursor lose a large amount of their incorporated water during the isothermal step, suggesting very weak interactions between the water and the polymer, whereas for the PDMS-PMHS-containing polymers, the main water loss takes place upon heating. The ability to take up a larger amount of water together with its slower release indicate that the water molecules are bound more strongly to the polymers formed from PDMS-PMHS than to the PMHS systems. The mass loss increases only slowly during heating for the polymers with additionally incorporated ethylene glycol groups, which suggests that these polymers bind the water most effectively.

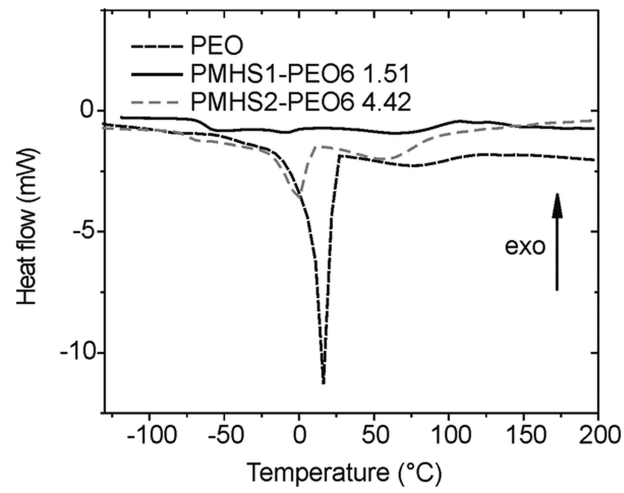

Figure 6. DSC thermogram of PMHS1-PEO6 1.51, PMHS2-PEO6 4.42, and allyl-terminated PEO.

Resulting from the non-co-continuous phases in this class of polymers, regions with high hydrophilicity are formed inside of the polymer system. These regions are ideal to immobilize metal ions and to model a growth limited precipitation environment for nanoparticles in the swollen state.

DSC and TGA. Investigations on the phase transitions and chain mobilities in the PEO/polysiloxane hybrid materials were carried out by means of DSC measurements, which were performed in a temperature range from −150 to 200 °C with a heating rate of 10 °C. Usually, this type of hybrid materials should exhibit a low T_g, which depends on the PEO chain length and is due to the crystallization of the PEO chains for chain lengths of 5−6 EO units and higher.[29] Crystallization in general was considered undesirable for the preparation of solid polymer electrolytes (SPE), which reveal some similarities to the prepared hybrid polymer matrices, as it was known as the main factor to decrease ion conductivity. In more recent works, however, it was shown that ionic conductivity exists in crystalline polymer electrolyte complexes under special conditions.[30] In our work, the inhibition of the crystallization of the PEO induced by the complexation of ions with the polyether oxygens is used as an additional proof for the immobilization of the ions at the PEO moieties. Pristine allyl PEO crystallizes and shows a melting peak at 17.9 °C (onset 0.9 °C, endothermic feature) (Figure 6). The typical 7/2 helical structure or the zigzag conformation is obtained upon crystallization of PEO.[31] Pure PMHS shows a T_g at −140.9 °C and pure PDMS-PMHS at −136.9 °C. Hybrid polymers consisting of low EO:Si ratios (e.g., 0.19) do not exhibit any detectable T_g (Table 2) in the temperature range from −150 to 200 °C. Furthermore, no crystallization of the PEO was observed, indicating a very rigid polymer network with reduced chain mobility. In the polymers with a PMHS backbone, the appearance of a glass transition temperature at approximately −60 °C was observed

(29) Lauter, U.; Meyer, W. H.; Wegner, G. *Macromolecules* **1997**, *30*, 2092–2101.
(30) Gadjourova, Z.; Andreev, Y. G.; Tunstall, D. P.; Bruce, P. G. *Nature* **2001**, *412*, 520–523.
(31) Takahashi, Y.; Sumita, I.; Tadokoro, H. *J. Polym. Sci., Part B: Polym. Phys.* **1973**, *11*, 2113–22.

Table 2. Results from Thermal Analyses for Selected Polymer Samples

polymer	T_g (°C)	melting peak onset (°C)	melting peak minimum (°C)	TGA mass loss
PMHS1-PEO6 0.19				25
PMHS1-PEO6 1.51	−58.0			53
PMHS1-PEO6 5.68	−62.9	−35.0	−20.1	74
PMHS2-PEO6 2.21	−72.0	−31.7	−10.8	84
PMHS2-PEO6 4.42	−70.8	−15.3	0.5	91
PMHS2-PEO6 1.77 eg	−88.5	−34.0	−19.5	72

with increasing EO content. This is in good agreement with literature values for similar cross-linked polymer systems, e.g., epoxy cross-linked polysiloxanes.[32] With increasing number of cross-linking sites, crystallization of the PEO chains takes place in the PMHS polymers, similarly to the PMHS2 polymers. The latter containing a block copolymer backbone exhibit a T_g, which is about 10 °C lower (at around −70 °C). This indicates the higher chain mobility in these systems and results also in the presence of the first-order phase transition of the PEO. Although this material reveals a rather high degree of cross-linking, the system is flexible enough to allow the ordering of the PEO chains to the typical 7/2 helical structure or the zigzag conformation.[33,34] The close vicinity of the PEO chains in the highly cross-linked systems (PMHS2-PEO6 4.42) facilitates crystallization, although the transition peak is broadened. The polymers having additional ethylene glycol groups also feature the crystallization peak of the PEO; however, the intensity is lower, because the shorter ethylene glycol chains induce a less-regular arrangement of the PEO chains. The polymers with additional ethylene glycol groups have the lowest degree of cross-linking and therefore the highest chain mobility together with the lowest T_g (−88.5 °C). Mass losses from TGA correlate with the amount of organics in the polymer. But one should be cautious with the interpretation, because the linear polysiloxanes form cyclic oligosiloxanes upon heating, which are volatile. This is more likely to occur in the case of the block copolymers. Therefore, they show mass losses higher than the expected amount calculated from the organic components.

Small-Angle X-ray Scattering (SAXS) Studies. SAXS measurements were performed to determine the different morphologies achieved by the application of the two polysiloxane backbones and the additional modification with small oligoethers. The SAXS-intensities were normalized to the second peak at higher q-values and show two broad peaks (Figure 7 and 8 for PMHS1 and PMHS2, respectively). Both peaks indicate a short-range order, i.e. a typical nearest neighbor-to-neighbor distance. The first peak at lower q-values is attributed to entangled polysiloxane chains, as the position of this peak depends on the chain length (larger distance of nearly 0.9 nm in real space for the larger chain length PMHS1 and about 0.7 nm for the smaller one,

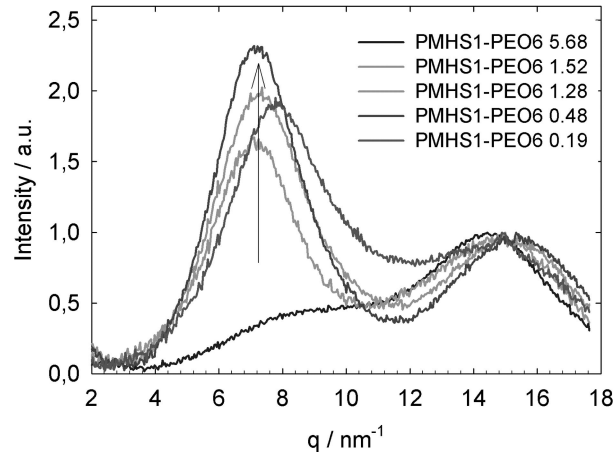

Figure 7. SAXS intensities in dependence on the scattering vector for PMHS1 with different silicon content, which is indicated by the arrow.

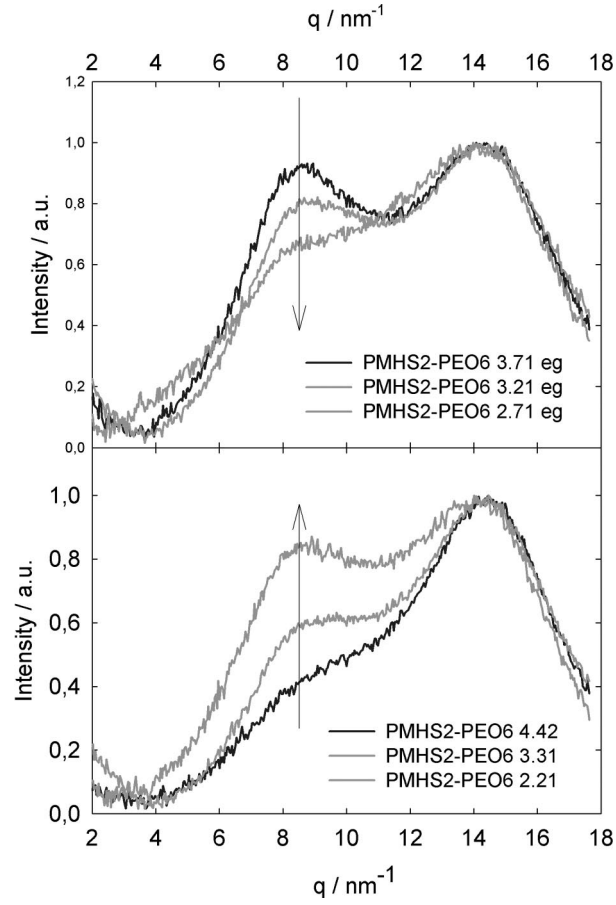

Figure 8. SAXS intensities in dependence on the scattering vector for (a) PMHS2 and (b) PMHS2 eg with different silica content. Increasing siloxane content is indicated by the arrows.

PMHS2). This is also supported by the literature,[35] where the entanglement of polysiloxane chains in hybrid polymers and the formation of spherical agglomerates (clusters) was observed, although occurring at larger distances. The second peak at about $q = 14.5$ nm^{-1} is independent of the size of the polysiloxane chains and therefore characterizes the distance of the polysiloxane chains with a spacing controlled by the cross-linking PEO. Increasing siloxane content is

(32) Liang, W.-J.; Kuo, C.-L.; Lin, C.-L.; Kuo, P.-L. *J. Polym. Sci., Part A: Polym. Chem.* **2002**, *40*, 1226–1235.
(33) Takahashi, Y.; Tadokoro, H. *Macromolecules* **1973**, *6*, 672–5.
(34) Vilkman, M.; Kosonen, H.; Nykaenen, A.; Ruokolainen, J.; Torkkeli, M.; Serimaa, R.; Ikkala, O. *Macromolecules* **2005**, *38*, 7793–7797.
(35) Dahmouche, K.; Santilli, C. V.; Pulcinelli, S. H.; Craievich, A. F. *J. Phys. Chem. B* **1999**, *103*, 4937–4942.

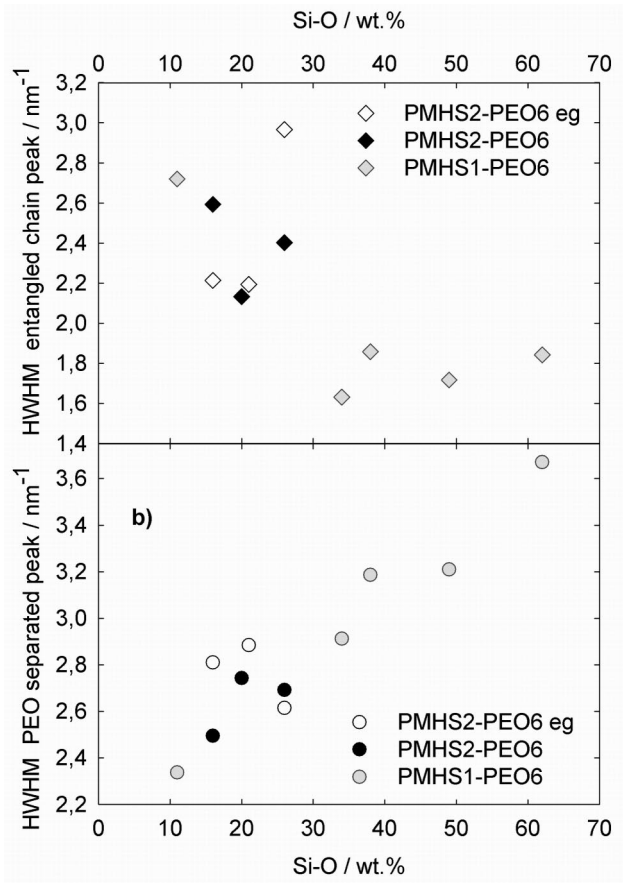

Figure 9. Half-width at half-maximum (HWHM) of the peak from entangled polysiloxane chains (peak at lower q-values) and the peak from PEO separated, cross-linked polysiloxane chains (peak at higher q -values).

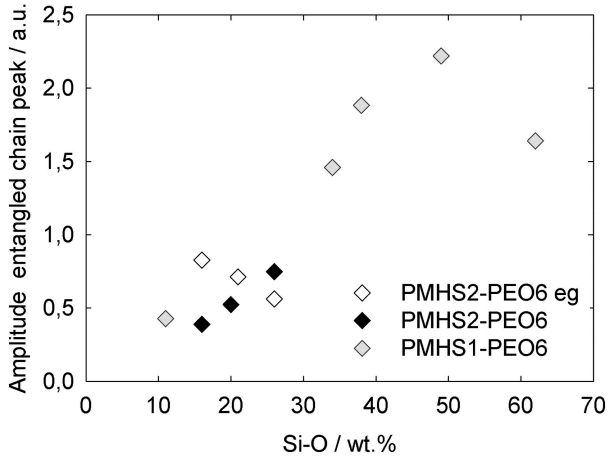

Figure 10. Amplitude of the peak from entangled polysiloxane chains (peak at lower q-values).

pointed out by the arrows in Figures 7 and 8. Although for PMHS1 (Figure 7) and PMHS2 (Figure 8a), an increase in the entangled polysiloxane peak with increasing siloxane content was observed, the opposite trend is visible for PMHS2 eg. This indicates a stronger influence of additional EO chains on the network formation in comparison to the amount of polysiloxane chains.

Both peaks were fitted with Gaussian functions and the numerical values of these fits are shown in Figures 9 and 10. The half-width at half-maximum (HWHM), Figure 9, of the entangled chain peak decreases whereas the HWHM

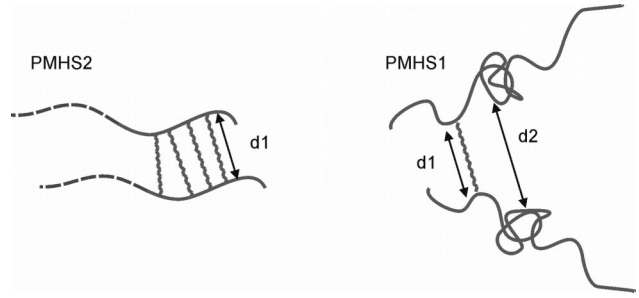

Figure 11. Schematic displays of distances found in SAXS; $d1 = 0.4$ nm and $d2 = 0.7$ or 0.9 nm for PMHS2 and PMHS1, respectively.

of the PEO-separated peak increases. The same behavior is observed for the positions of the maxima in q-space, thus these data are not shown for brevity. This clearly indicates that both processes, the entanglement of polysiloxane chains as well as the separation and cross-linking with PEO, are competing with each other to control the morphology of the polymer.

The amplitude of the entangled chain peak at lower q-values increases with increasing siloxane content (Figure 10). Only at the highest siloxane content, a decrease is observed. As already mentioned above, the opposite trend in the amplitude of PMHS2 and PHMS2 eg indicates the stronger influence of additional EO chains on the network in comparison to a higher amount of polysiloxane chains.

It is very probable that the two competing processes are on the one hand the formation of entangled polysiloxane clusters (the peak at lower q-values dominates) and on the other hand the cross-linking and bridging of the polysiloxane chains with PEO, which leads to a more linear and closer arrangement of the polysiloxane chains (the peak at higher q-values dominates). This is also supported by the increasing intensity of the entangled polysiloxane cluster peak with a typical size (Figure 11) of nearly 0.9 nm for PMHS1 and 0.7 nm for PMHS2 with increasing siloxane content (Figure 10) in relation to the PEO chain peak with a smaller size of approximately 0.4 nm (Figure 11).

In the case of PMHS1, the amplitude of the entangled polysiloxane peak is very low for the highly cross-linked PMHS1-PEO6 5.68 and increases strongly with increasing siloxane content, which characterizes a transition from a more linear and cross-linked morphology of the polymer to a polysiloxane entanglements arrangement with a nanophase separation. The peak amplitude decreases only for the highest siloxane content, probably because of sterical hindrance of the polysiloxane chains themselves.

In the case of PMHS2, the morphology of the polymer is slightly different, probably because the formation of spherical polysiloxane clusters is less pronounced for a smaller polymer. However, a correlation of increasing peak amplitude with increasing siloxane content is visible for PMHS2 in Figure 8a (visualized by the arrow) and Figure 9a. Contrary to PMHS2, in the additionally functionalized copolymer PMHS2 eg, the peak intensity decreases with increasing Si-content (Figures 8b and 9b). The reason for this surprising behavior is probably that the additionally added ethylene glycol chains contribute to the EO:Si ratio but do not serve as cross-linkers. These small glycol chains seem to inhibit

an arrangement of the PEO chains and foster siloxane cluster formation, and their effect is considerably stronger than an increase in the amount of siloxane chains.

Infiltration with Fe(II) and Fe(III) Ions. Previous studies on siloxane−PEO hybrid materials formed of an end-modified oxyethylene-co-propylene precursor that is applicable in the sol−gel process are reported in the literature. Those polymer systems could host different metal ions, e.g.: Fe(II) and Fe(III). In this case, the doping takes place during the sol−gel process, and thus network formation might be disturbed by a coordination of the metal ions to the ethylene oxide chains. In our study the cross-linked polysiloxanes were infiltrated with Fe(III) and Fe(II) solutions in water. An aqueous ammonia solution was added to initiate the formation of oxidic nanoparticles.[36,37] The nanoparticles were prepared in the swollen and infiltrated polymer that forms hydrophilic regions depending on the swellability of the polymeric matrix. Fe(II) ions were used because of their distinct coloration, so the infiltration (green, yellowish) and the precipitation (red-brown) process could be followed visually.

The IR-spectrum of the PMHS2-PEO6 4.42 infiltrated with $FeCl_2$ solution (0.25 M/water) shows the characteristic vibrations of the cross-linked hybrid polymer. Residual Si−H bonds were hydrolyzed during this process resulting in an OH vibration at 3360 cm^{-1}. No cleavage of the other polymer bonds could be observed during infiltration and precipitation. A coordination of surface Fe^{2+} ions of the nanoparticles after precipitation by the oxygens of the PEO chains can not be affirmed by FT-IR, because of a low ion concentration in the doped sample leaving many PEO oxygens unbound to metal ions and leading to spectra dominated by the uncoordinated PEO chains. In similar polymer systems doped with Fe(II), it was shown that the coordination takes place via the oxygens of the PEO chains.[38] The PEO chains strongly interact with the Fe ions and a coordination by the ether oxygens is most likely. The ions are immobilized at the hydrophilic regions in the polymer matrix, which restrict the nanoparticle growth in the nanoparticle preparation step. Direct evidence is difficult to obtain because of the limited solubility of the polymer matrix and exclusion of NMR spectroscopy as an analytical tool. Currently the binding and growth of lanthanide-based nanoparticles is the object of our investigations. In these cases, we can definitely show applying spectroscopic techniques that the ion binding and particle growth occurs in direct contact to the PEO chains. This will be the topic of a subsequent publication.

The stability of the polymer bonds is also supported by TGA measurements, which did not show any alteration of the onset temperatures (250 °C) compared to the pure polymer sample. Furthermore, the overall mass loss was decreased by 11 wt % compared to the pristine polymer matrix. However, this value cannot be used for the determination of the amount of infiltrated Fe(II) because of the formation of cyclic polysiloxanes during heating which can be influenced by the presence of the iron oxide. DSC of the polymer samples infiltrated with the Fe-chlorides followed by a precipitation step did not show any recrystallization of the PEO, which is due to the sterical hindrance by the nanoparticles and a possible coordination to the nanoparticles surface. Similar behavior was observed in literature before when Fe_3O_4 particle were incorporated into a SPE to enhance ion conductivity by inhibition of the recrystallization of the PEO chains.[39] Additionally, an increase in the T_g was observed because of the decrease in chain mobility, because the nanoparticles act as obstacles on the mobility of the chains. From systems that consist of only Fe(II) ions, mainly FeO is formed, shown by XRD. The polymer matrix is completely amorphous giving the typical amorphous silica band between $2\theta = 15°$ and 25°, but the nanocrystalline phase indicated by the small but broadened reflexes could be identified as FeO (JCPDS 6−615), together with a slight reduction of the size of the elementary cell (see the Supporting Information). The sharp diffraction peaks at $2\theta = 15°$ and 28° are most probably due to small quantities of ammonium iron chloride.

The successful infiltration of the polymer samples with Fe-chloride solutions is also supported by EDX analysis

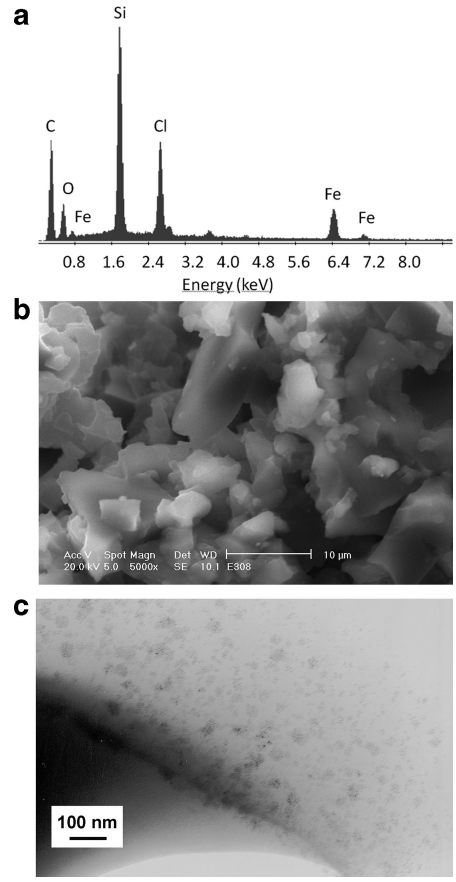

Figure 12. EDX analysis and SEM image of PMHS2-PEO6 4.42 infiltrated with $FeCl_3$ and precipitated with ammonia solution, TEM image of PMHS2-PEO6 3.3 infiltrated with $FeCl_2$ and precipitated with ammonia solution.

(36) Koo, H. Y.; Chang, S. T.; Choi, W. S.; Park, J.-H.; Kim, D.-Y.; Velev, O. D. *Chem. Mater.* **2006**, *18*, 3308–3313.
(37) Moore, R. G. C.; Evans, S. D.; Shen, T.; Hodson, C. E. C. *Physica E* **2001**, *9*, 253–261.
(38) Silva, N. J. O.; Amaral, V. S.; Bermudez, V. d. Z.; Nunes, S. C.; Ostrovskii, D.; Rocha, J.; Carlos, L. D. *J. Mater. Chem.* **2005**, *15*, 484–490.
(39) Reddy, M. J.; Chu, P. P.; Kumar, J. S.; Rao, U. V. S. *J. Power Sources* **2006**, *161*, 535–540.

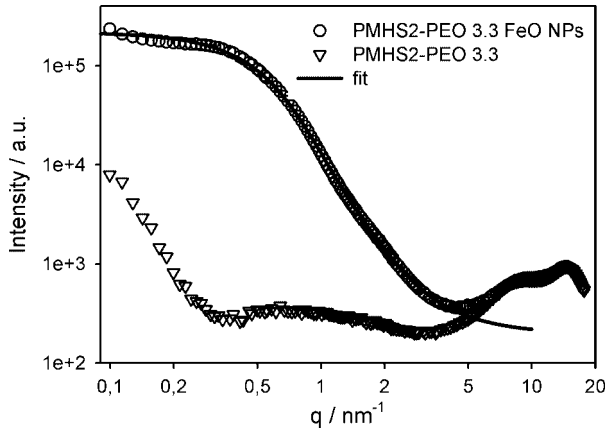

Figure 13. SAXS pattern of PMHS2-PEO6 3.3 (triangles) and PMHS2-PEO6 3.3 infiltrated with Fe(II) and precipitated (circles). The line is a fit for randomly distributed spheres with a Gaussian size distribution.

(Figure 12). Besides Fe ions, Cl ions were found because of incomplete hydrolysis of the $FeCl_3$ precursor. No EDX signal corresponding to Pt was observed, indicating that no residues of the hydrosilation catalyst were present in the samples. In the corresponding SEM image the homogeneous polymer is displayed, showing no precipitation on the surface of the polymer. This leads to the conclusion that the Fe-ions are located within the hybrid polymer matrix. In the TEM, the FeO nanoparticles with a diameter ranging from 10 to 20 nm are visible (Figure 12). The nanoparticles are found mainly at the boundaries of the polymer samples, which is due to the fact that only these regions were sufficiently thin to be transparent for the electron beam.

Figure 13 shows the SAXS intensities of the material (PMHS2-PEO6 3.3) without nanoparticles (triangles) and with nanoparticles (circles) from infiltration and precipitation with Fe(II). The intensity at large q-values arises from the polysiloxane chains and the polymer. Towards low q-values, a strong additional SAXS contribution from the nanoparticles is observed, which arises from the high electron density contrast between particles and matrix. The fit (line) describes randomly distributed spheres with a diameter of 8.4 nm and a Gaussian distribution with a Gaussian half-width of 2.2 nm. This nanoparticle diameter calculated from SAXS (8.4 $\pm$ 2.2 nm) is smaller than the particle diameters observed in the TEM images. In the low-resolution TEM image, only the larger particles or agglomerates are visible, whereas in SAXS, a statistically firm mean value of all particles is determined.

Conclusion

Hybrid polymers were prepared with varying EO:Si content based on two different polysiloxane backbones. The polymers were additionally functionalized with short pending ethylene glycol chains to increase ion binding properties. EO:Si ratios designed ranged from 0.06 up to 5.68. The defined structure of the hybrid polymers allowed the swelling with apolar and polar solvents. The highest swelling degrees were achieved with methanol. For all polymer samples high swelling degrees were obtained for high EO:Si contents. Even the very hydrophilic polymers were able to incorporate amounts of toluene ranging up to their own weight. The cross-linked polymers feature glass transition temperatures of around -70 °C for the block copolymer and -60 °C for the polymers made from PMHS. The crystallization of the PEO in the polymers having the PMHS backbone is inhibited due to a rigid polymer backbone and long distances between the PEO. The investigations with SAXS revealed that two competing components, the cross-linking PEO chain and the entanglements of the polysiloxane chains, determine the morphology of the polymer. If the PEO chains dominate, the polysiloxane chains were forced into a linear arrangement, whereas in the opposite case, the polysiloxane chains form entangled clusters with a short-range order.

The metal coordination sites of the PEO chains enabled the introduction of metal ions into the cross-linked polymer. The good swelling ability of the matrix together with its hydrophobic/hydrophilic nature led to the formation of areas able to limit nanoparticle growth. Fe-oxide nanoparticles with a diameter of 8.4 nm $\pm$ 2.2 nm were successfully introduced into these polymers by an infiltration approach, and the polymer matrix was used to inhibit further growth of these particles.

Acknowledgment. Financial support of this work by the Austrian Fonds zur Förderung der wissenschaftlichen Forschung (FWF, Project P17731) is gratefully acknowledged. We thank the University Service Center for TEM (USTEM) Vienna for the help in production of TEM images. In addition, we thank Dr. Thomas Koch and Dr. Erich Halwax for measurements and fruitful discussions.

Supporting Information Available: Information about FT-IR spectroscopic data, TGA and XRD of the FeO nanoparticle containing samples, and diagrams explaining the swelling behavior (PDF). This material is available free of charge via the Internet at http://pubs.acs.org.

CM802171S